ELSEVIER

Contents lists available at ScienceDirect

Environmental Pollution

journal homepage: www.elsevier.com/locate/envpol



Remediation of contaminated sediments containing both organic and inorganic chemicals using ultrasound and ozone nanobubbles*



Shaini Aluthgun Hewage, Janitha H. Batagoda, Jay N. Meegoda

Department of Civil & Environmental Engineering, New Jersey Institute of Technology, Newark, NJ, 07102, United States

ARTICLE INFO

Article history:
Received 2 November 2020
Received in revised form
2 January 2021
Accepted 17 January 2021
Available online 25 January 2021

Keywords:
Sediment remediation
Contaminants
Organic
Heavy metals
p-terphenyl
Chromium
Ultrasound
Ozone
Nanobubbles

ABSTRACT

Most river sediments are contaminated with organic and inorganic pollutants and cause significant environmental damage and health risks. This research is evaluated an in-situ sediment remediation method using ultrasound and ozone nanobubbles to remove organic and inorganic chemicals in contaminated sediments. Contaminated sediment is prepared by mixing synthetic fine sediment with an organic (p-terphenyl) and an inorganic chemical (chromium). The prepared contaminated sediment is treated with ultrasound and ozone nanobubbles under different operating conditions. For the samples with the maximum initial concentration of 4211 mg/kg Cr and 1875 mg/kg p-terphenyl, average removal efficiencies are 71% and 60%, respectively, with 240 min of sonication with 2-min pulses, whereas 97.5% and 91.5% removal efficiencies are obtained for the same, respectively, as a single contaminant in the sediment. For the same maximum concentrations, the highest removal of p-terphenyl is 82.7% with 127.2 J/ml high energy density, and for Cr, it is 77.1% using the highest number of the treatment cycle and ozone usage with 78.75/ml energy density. The Cr highest removal efficiency of 87.2% is recorded with the reduced initial concentration of 1227 mg/kg with the highest treatment cycles. The Cr removal efficiency depends on the availability of oxidizing agents and the number of washing cycles of sediments, whereas P-terphenyl degradation is most likely influenced by the combined effects of oxidation and ultrasound-assisted pyrolysis and combustion of organics.

© 2021 Elsevier Ltd. All rights reserved.

1. Introduction

Background. Worldwide most river and lake sediments are contaminated with organic and inorganic pollutants (Wuana et al., 2014). River sediments act as a sink or reservoir for industrial, agricultural, or other sources of pollution and are subjected to sediment contamination (Yong, 1995). The United States Environmental Protection Agency (USEPA) stated that sediments are a common cause of contamination of freshwater bodies, and these contaminated sediments cause environmental damage accounting for over \$16 billion per year (USEPA, 2019).

The lower Passaic River, NJ, USA, has been identified as being one of the heavily contaminated river with high concentrations of toxic, persistent, and bioaccumulative organic and inorganic chemicals due to a century of industrial activities (USEPA, 2014a). Those contaminants pose extreme human and ecological risks.

E-mail address: meegoda@njit.edu (J.N. Meegoda).

Humans are exposed to those contaminants in sediments because of the consumption of fish and crab from the river. Over 100 current and former industrial facilities have been recognized as potentially liable for discharging a number of contaminants to the river, including but not limited to dioxins and furans, PCB mixtures, PAH compounds, DDT, and other pesticides, and chromium mercury, lead, and other metals. The distribution of contaminants concentrations is widely varied along the river from location to location. In general 2,3,7,8-TCDD (pg/g) 0.09-34,100, Total TCDD (pg/g) 2.2-37,900, Total PCBs ($\mu g/kg$) 0.1-28,600, Total DDx ($\mu g/kg$) 0.32-10,229, Dieldrin (µg/kg) 0.01-152, Chlordane (µg/kg) 0.05-254, Total PAHs (mg/kg), 0.21-2806, Mercury (mg/kg) 0.05-16, Chromium (mg/kg) 224-584, Copper (mg/kg) 0.21-2470, Lead (mg/kg) 4.4-609 and other organic and heavy metals have been found in the first 6 inches of surface sediment samples (Louis Berger Group, 2014: Onwueme and Feng. 2006).

The USEPA has declared the lower Passaic River as a Superfund site and in 2014, the USEPA proposed an ex-situ remediation plan consisting of mechanical dredging, dewatering, and secure disposal for the first 9 miles of the contaminated sediments in the River

^{*} This paper has been recommended for acceptance by Jörg Rinklebe.

Corresponding author.

(USEPA, 2014b). Recently the USEPA is also investigating spot treatment of Passaic River upstream of the 9 mile marker (USEPA 2014b). Above is considered an expensive solution and expected to be completed in 5 years. It would greatly impact the socioeconomic growth of Newark and surrounding areas by closing and opening of draw bridges to pass barges carrying dredged sediment and establishment of a sediment processing facility. To mitigate these concerns of the USEPA proposal, the in-situ remediation method described below is proposed.

There is limited research on remediation methods to treat soils/sediments contaminated with both organic and inorganic contaminants. Mostly, evaluation of soil/sediment treatment methods has addressed individual contaminants and not both organic and inorganic pollutants. Due to the significant difference between the environmental, chemical, and physical behavior of heavy metals and organic pollutants in sediments, finding a remediation method for treating both types of contaminants pose a significant challenge. The USEPA has summarized the currently available in-situ treatment technologies for organic and inorganic contaminants, and it only shows the effectiveness of different treatment methods for different contaminant types (USEPA, 2006) but not for combined organic and inorganic contaminants.

This research develops a novel and innovative in situ remediation method that can remediate heavily contaminated sediments (both organic and inorganic) by the combined effects of ultrasound, ozone, and nanobubbles. This manuscript presents the third stage of a comprehensive investigation. In the first two stages, applicability of this method for a single contaminant in the sediment was evaluated (Aluthgun Hewage et al., 2020; Batagoda et al., 2019). The next stage would be the treatment of actual river sediments and then eventual in-situ implementation.

Hypothesis. The ex-situ treatment methods for contaminated revier sediments are not always feasible, requiring a low-cost insitu treatment technolgy that can remediate the contaminated sediments. Sediments are found to be contaminated by various chemical compounds that require viable treatment methods with the capacity to treat both the organic and inorganic compounds simultaneously. There are very few studies on sediment remediation containing a mixture of organic and inorganic contaminants than single contaminant types (organic or inorganic). It is hypothesized that the treatment of sediments containing both organic and inorganic contaminants would not be substantially reduced due to interactions, when compared to the individual treatment efficiencies of either organic or inorganic contaminants.

Research objectives. A sediment contaminated by organic pterphenyl and inorganic chromium was used to evaluate the proposed treatment method. Therefore, the prepared contaminated sediment was treated with ultrasound and ozone nanobubbles under different operating conditions to obtain optimal treatment efficiency under laboratory conditions.

2. The development of the treatment method

A contamination treatment is expected to destroy, remove, immobilize, isolate, or detoxify the contaminants (USEPA, 1991). The treatment methods can be divided into two categories, in-situ and ex-situ treatment techniques. In general, in-situ treatment methods have significant cost advantage when compared to ex-situ methods, but ex-situ treatment methods have higher treatment efficiencies. However, in-situ remediation methods are more viable for larger contaminated sites concerning cost and socio-economic impact on the region (Thomé et al., 2019).

In-situ Treatment Technologies. Although there are many treatment methods available for in-situ soil and sediment treatment, selecting a suitable treatment method depends on site

characteristics, treatment cost, specific objectives, required levels of treatment, and external environmental impacts. In-situ treatment can be mainly divided into five categories (Thomé et al., 2019; USEPA, 2006); (1) physical, (2) chemical, (3) biological, (4) thermal, and (5) combined. For the lower Passaic River, a treatment method for the river sediment at the river bottom is needed. Hence, most of the above treatments are inapplicable, leaving chemical oxidation as the most feasible option with respect to applicability and cost. Therefore, an appropriate oxidizer should be selected that can treat both organic and inorganic contaminants.

The proposed in-situ treatment method is explained in previous publications (Aluthgun Hewage et al., 2020; Batagoda et al., 2019; Meegoda et al., 2017a). This technology will be implemented from a barge, and the sediment treatment chamber will be lowered to the river bottom using a crane, as shown in Fig. 1. The treatment chamber is designed so that the generated wastewater does not contaminate the surrounding environment and is directly extracted to the wastewater treatment facility on the barge. The extracted wastewater is treated utilizing nanofiltration and subsequent precipitation before releasing back to the chamber with fresh nano ozone. In addition to the wastewater treatment facility, the barge contains the ozone generator and nano-ozone bubble generator. Once the barge treatment system with all the above is installed, the system will only need chemicals to treat wastewater, power, and oxygen obtained from the air. The power for the system will be generated using solar panels. Hence there is no additional operation cost to treat the river sediments other than chemicals used for wastewater treatment. The proposed in-situ treatment chamber depicted in Fig. 1 for field implementation is $10' \times 10' \times 5'$ size and details are described in previous publications (Aluthgun Hewage et al., 2020; Batagoda et al., 2019; Meegoda et al., 2017a). This technology can be easily used for the proposed USEPA spot treatment of upstream of the 9-mile marker of the Passaic River (USEPA 2014b). Several systems as shown in Fig. 1 may also be deployed to expedite the Passaic River remediation. Meegoda and Perera (2001) and Meegoda and Veerawat (2002) showed that ultrasound could desorb both organic and inorganic contaminants attached to sediments. Ozone is applied to prevent re-adsorption of organics by mineralization and to prevent re-adsorption of inorganics by oxidizing and solubilization. Treated and solubilized inorganics are removed by the wastewater treatment unit on the barge.

Selection of an oxidizing agent. As stated before, chemical oxidation is one of the promising treatment methods that has been utilized to treat both organic and inorganic pollutants. It has the capability of not only mineralize organic contaminants but also reducing their toxicity. However, depending on the solution chemistry, the toxicity of metals can increase or decrease with chemical oxidation (Sharma et al., 2018). The most commonly used oxidizing agents are ozone, hydrogen peroxide, hypo-chlorites, chlorine, permanganate, and chlorine dioxide (Kuppusamy et al., 2016; Teefy, 1997). Also, advanced oxidation processes (AOPs) which involve the use of hydroxyl radicals OH^{\bullet} (oxidation potential, 2.80 V) have been widely investigated by researchers in recent years as an effective oxidizing agent.

For this research, ozone was selected as the oxidizing agent because it has many advantages over other oxidizers. Most of the oxidizers listed earlier are either too costly, localized, have a very short half-life, or are new technologies that are not well established. Moreover, ozonation can also be considered as an AOP in soil treatment as it involves the formation of OH^{\bullet} radicals due to the indirect reactions formed by the degradation of ozone.

Ozone as an oxidizer. Ozone reacts readily with organic and inorganic substances (Loeb et al., 2012). It is a powerful oxidant that has been used in the chemical industry. Ozone has one of the highest oxidation potentials of any substance (2.07 V), exceeded

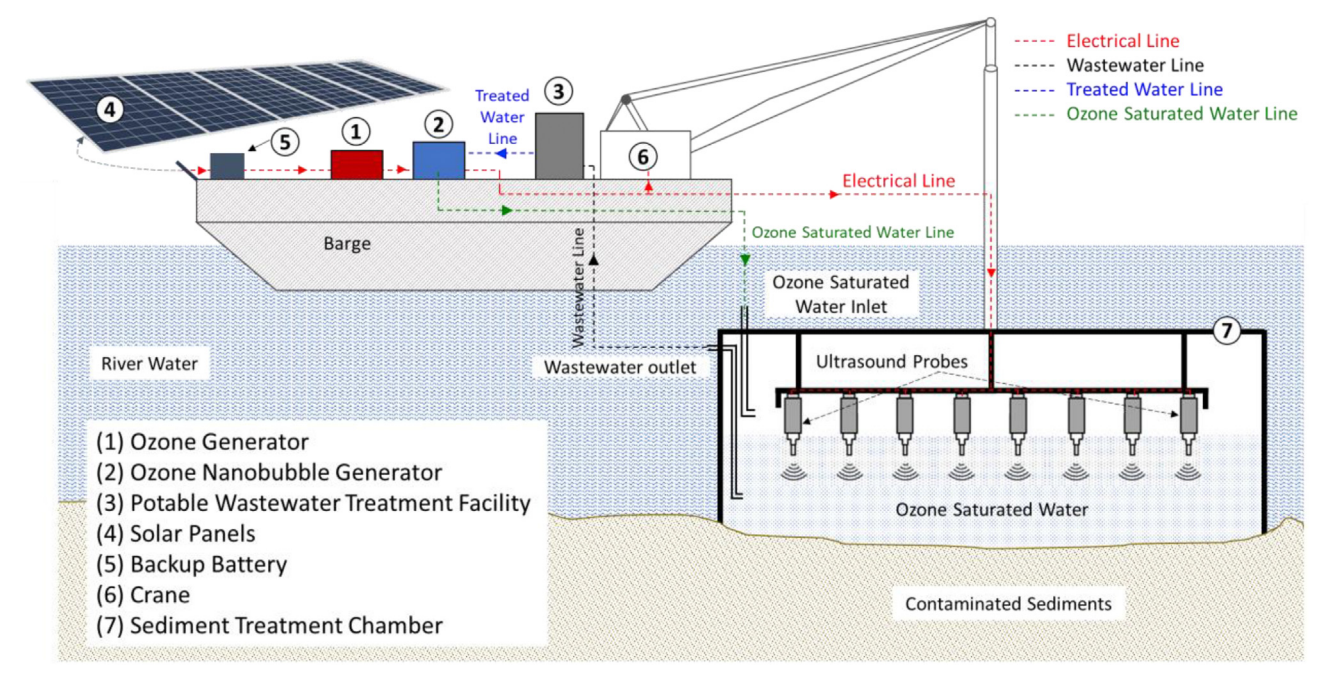


Fig. 1. The systematic diagram of the proposed treatment method for field implementation.

only by fluorine (2.87 V), hydroxyl radicals (2.86 V), and oxygen atoms (2.34 V) (Yang and Zhu, 2016). Ozone treatment includes direct and indirect reactions (Eriksson, 2005; Rasalingam et al., 2014). Indirect oxidation is due to the disintegration of ozone in water to OH and radicals (Batagoda et al., 2018). With the formation of OH^{\bullet} radicals, successive reaction chains are created that yield H_2O_2 and OH•, among other radicals (Batagoda et al., 2018; Krishnan et al., 2017). Many factors control the stability and half-life of aqueous ozone. They include ozone concentration, temperature, pH, hydroxyl radicals, movement or stirring of the liquid, and the availability of organic and inorganic substances (Batagoda et al., 2018). Ozone can be inexpensively generated from the air. The stability (i.e., contact time), ozone concentration, and hydroxyl radical formation are essential factors that control the oxidation's efficiency. The solubility of ozone in water is relatively low, so ozone delivery to the aqueous solution can be improved using ozone nanobubbles (Hu and Xia, 2018).

Application of nanobubbles. In general, bubbles are defined based on their size (diameter); macro-bubbles (>100 μm), microbubbles (1 μ m -100μ m), and nano8bubbles (<1 μ m) (Chaplin, 2019). Nanobubbles have a diameter smaller than 200 nm (Agarwal et al., 2011; Ebina et al., 2013; Meegoda et al., 2018). The industrial application of nanobubble technology has exponentially increased over the past two decades due to their long-term stability and reactivity (Liu et al., 2013; Ushikubo et al., 2010). Due to their extremely small size, high internal pressures, high specific area, and long stagnation times, they have improved the mass transport from gases in bubbles to liquids. Nanobubbles have an electrically negetive charged interface that facilitate the physical adsorption, expediting the chemical reactions at the gas-liquid interface compared to ordinary and microbubbles (Hu and Xia, 2018; Meegoda et al., 2018). Further, the surface charges reduce bubble coalescence and improve bubble stability due to electrostatic repulsion (Hewage et al., 2021; Meegoda et al., 2018).

However, in order to have contact between soil contaminants and the ozone nanobubbles, soil should be in a suspension, and contaminants must be desorbed from the sediments. The ultrasound can produce such desorption of contaminants from the sediments and maintain the sediment in suspension (Meegoda and Perera, 2001; Meegoda, and Veerawat, 2002).

Application of ultrasound. In this research, the primary purpose of ultrasound is to agitate the soil, keep the soil in suspension, and desorb contaminants from sediments. Depending on the applied power and frequency of ultrasound, bonds between the soil and the contaminants break due to mechanical shearing induced by ultrasound. This shearing force is developed due to a phenomenon known as acoustic cavitation. During cavitation, vapor bubbles are generated, and they obtain an ample amount of energy from sound waves. This aguired energy concentrates inside the bubble as kinetic energy, and when bubbles become unstable, they implode. This implosion can erode solids, initiate chemical reactions, and produce radicals (Young, 1999). Therefore, the sonication is a combination of sonochemical and sonophysical effects. The chemical effects are due to the localized high temperatures and pressures generated during bubble implosion. This results in the thermolysis of chemicals and the formation of radicals such as OH• and H[•] (Flint and Suslick, 1991). The sono-physical effects, such as shock waves produced by the cavitation of bubbles result in turbulent fluid/slurry movements and a higher microscale velocity gradient near the vicinity of cavitation (Chen et al., 2011). The shock waves created during bubble implosion can break particles and macromolecules; for macromolecules, this is referred to as shear degradation by ultrasound (Kewalramani et al., 2020).

The yield of sonication treatment of soil depends on energy dispersed by ultrasonic waves, soil, and contaminant properties. The power and frequency control the energy dispersed by ultrasonic waves. A higher power intensity leads to higher acoustic pressures (amplitude and vibration), much more cavitations, and violent cavitational collapses. Compared to higher frequencies of ultrasound, low-frequency ultrasound produce a lower number of bubbles, larger resonant bubble size, and more violent bubble collapse (Chen et al., 2011). Typically, low-frequency ultrasound has strong sono-physical effects compared to high-frequency ultrasound. High-frequency ultrasound promotes more sonochemical reactions due to increased cavitational bubble events and the associated formation of OH• radicals (Meegoda and Kewalramani,

2020).

The purpose of ultrasound in this research is to aid the mechanical agitation and desorption of contaminants from the soil particles. Accordingly, low frequency (20 kHz) ultrasound with optimum power levels was selected for this treatment process.

3. Materials and methods

Soil Preparation and contamination. The sediments from the Passaic River contain many different organic and inorganic contaminants in various concentrations. To evaluate the treatment process and to optimize, a controlled environment is needed. Therefore, it was decided to use synthetic sediments contaminated with one organic and one inorganic compound.

Preparation of the synthetic soil. The synthetic soil was prepared based on the actual size distribution of Passaic River sediments. The particle size distribution of synthetic soil and the dredged river sediment sample can be found (Aluthgun Hewage et al., 2020; Batagoda et al., 2019; Hewa Batagoda, 2018). The average size distribution of Passaic River sediments showed that on average, there were 15% clay and 62% silt contents, yielding a total fine fraction of 77%. Hence the laboratory synthetic soil consisted of mixture of kaolin, slit, rock flour, and fine sand. Table 1 shows the composition of this synthetic soil. Please note that all soil types or components listed in Table 1 are commercially purchased with near-zero organic carbon contents.

Organic contaminant. P-terphenyl ($C_{18}H_{14}$) was selected to represent the organic contaminant. This compound was selected to mimic the properties of PAH contamination as it has lower toxicity and is less hazardous, a consideration that ensured the safety of the research personale. The appropriateness of the selection of p-terphenyl to represent PAH has been previously explained (Aluthgun Hewage et al., 2020). The p-terphenyl is a white or light-yellow compound that appears in the form of needles. It has a molecular weight of 230.31 g/mol, a melting point of 213 °C, a boiling point of 376 °C, and is insoluble in water. When compared, PAHs have molecular weights of 152.21–276.34 g/mol, melting points of 93–278 °C, and boiling points of 270–496 °C.

Inorganic contaminant (heavy metal). Chromium was selected as a representative heavy metal contaminant as it is one of the most challenging metal contaminants to decontaminate. Lin and Chen showed the ability to adsorb heavy metals into sediments increased in the order Zn < Pb < Cu < Cr, and typically concentration of adsorbed Cr in sediments is much higher than that for other metals (Lin and Chen, 1998). Hence, Cr facilitates the understanding of the applicability of the proposed technology and can extrapolate the possibility of removing other metal contaminants, which are comparatively easier to remove than chromium.

Chromium is present in many forms in the nature, yet there are two primary stable chromium forms: trivalent and hexavalent chromium or Cr(III) and Cr(VI). The trivalent chromium is not water-soluble, while hexavalent chromium is water-soluble over a wide range of pH values (Kamolpornwijit et al., 2015). Even though the Cr(III) is not water-soluble, its sorption properties cause it to

seep into the soil and eventually release as Cr(VI) (Kamolpornwijit et al., 2015).

In the proposed field treatment setup, due to the application of ultrasound, heavy metals desorbed to sediments are released to wastewater. However, after the ultrasound is terminated, those desorbed heavy metals can get re-adsorbed. Any selected heavy metal would be desorbed from the sediments due to the applied ultrasound, but to prevent re-absorption, it necessary for them to stay as a soluble form. This can be accomplished by either oxidation or pH adjustment. The selection of chromium helped the removal of Cr due to Cr(III) oxidation to Cr(VI) increase the solubility. The Cr(VI) in the wastewater is subsequently removed by nanofiltration/precipitation.

Hence, in this research, trivalent chromium was used to represent heavy metal contaminants. The treatment protocol proceeds as follows. The desorption of contaminants from the soil occurs due to the application of ultrasound. The ozone oxidized the contaminant in the solution, allowing the trivalent chromium to become hexavalent, thereby becoming soluble in water and easier to remove from the soil water mixture with nanofiltration. However, Cr (VI) has to be carefully handled as it is 100 times more toxic than Cr (III). Cr (VI) is included in the list of class "A" human carcinogens by the USEPA (Kamolpornwijit et al., 2018; Meegoda et al., 2017b; Richard and Bourg, 1991). It was also found that chromium in clay is immobile and stable, which requires substantial energy for decontamination (Meegoda and Perera, 2001).

Preparation of Contaminated Sediments. In order to prepare contaminated sediments, 80 g of synthetic soil were mixed with 1 g of $CrCl_3 \bullet 6H_2O$. The chromium-contaminated dry soil was mixed with 0.15 g of p-terphenyl. The following section describes the soil preparation.

A 1.0 g of $CrCl_3 \bullet 6H_2O$ was dissolved in 50 ml of deionized (DI) water. This solution was then mixed with the 80 g of synthetic soil for 1 h using a mechanical mixer. The sample was placed in an oven at 40 °C for 24 h to evaporate water. This sample was then kept in a high-temperature oven at 800 °C for 3 h under an oxygen-free environment (under the nitrogen gas supply) for adsorption and to create proper bonds between soil and the chromium. The oxygen-free environment was maintained to ensure that the chromium would not become oxidized during heating. After 3 h, the oven was turned off, but the nitrogen gas supply was maintained until the samples reached room temperature.

The chromium contaminated soil is then mixed with p-terphenyl. To do so, 0.15 g of p-terphenyl was measured and dissolved in 50 ml of acetone (certified ACS reagent grade with \geq 99.5% purity) for 2 h to ensure complete dissolution. The previously prepared 80 g of chromium-contaminated soil was then mixed with the p-terphenyl solution for another 2 h until the acetone evaporated and p-terphenyl was absorbed into the soil matrix. This sample was then further mixed to ensure even distribution of contaminants. This uniformly contaminated soil was air-dried for 24 h before use.

According to the previous studies with a single contaminant in soil (Aluthgun Hewage et al., 2020; Batagoda et al., 2019), the

Table 1Composition of the synthetic soil (Aluthgun Hewage et al., 2020).

Soil Type	Percent of Soil	Other Properties
Sand (>75μ m)	2.60	Water Content = 3.6% pH ≈ 7 and negligible organic carbon content
Silt	4.62	
Rock Flour	20.24	
Kaolin	1.45	
Rock Flour (<75 μm)	71.09	
Total	100.00	

supplied ozone was fully utilized. Therefore, theoretically, with two contaminants in the soil, the ozone concentration demand should be doubled. However, with the solubility limit of ozone nanobubbles and limitation of laboratory facilities, such ozone concentration was not possible. Therefore, for selected experiments, contaminant concentration was reduced to 1/2 or 1/3 of the values mentioned above (1 g of Cr and 0.15 g of p-terphenyl in 80 g of soil).

4. Experimental setup

The main experimental procedure can be described by six steps: (1) preparation of the synthetic sediment, (2) sediment contamination, (3) ozone nanobubble generation, (4) soil treatment using ozone nanobubbles and ultrasound, (5) chemical analysis, and (6) data processing to calculate the removal efficiencies. This treatment process adopted in this research is shown in Fig. 2.

Generation of Ozone Nanobubbles. Nanobubbles were generated in a 25 L container filled up to 18 L. Hydrodynamic cavitation method was used to generate ozone nanobubbles. The BT-50FR micro-nano-sized nozzle was used to form nanobubbles, and a 380 kPa water pump was used to circulate water through the nozzle. In the nozzle, water was pumped into the nozzle at a tangential direction to form a swirled flow inside the vessel. This generated a flume of micro and nanobubbles in water. Nanobubbles were generated for 6 min, while ozone gas was supplied. Ozone gas was produced by passing the oxygen gas (provided by the compressed gas cylinders with regulators) through an Ozonator (A2Z Ozone MP - 3000 Multipurpose Ozone Generator). The details of nanobubble generation can be found (Aluthgun Hewage et al., 2020; Batagoda et al., 2019).

Treatment of sediments using ozone nanobubbles and ultra-sound. The 80 g of prepared contaminated sediments were placed inside the treatment chamber. The chamber was constructed using high-density polycarbonate (transparent) shell walls and a high-density polyethylene base, as shown in Fig. 3. The total volume of the chamber was 3.5 L. The base of the chamber was made of conical shape to enable the sediments to settle and accumulate at the bottom of the chamber. The outlet for the effluent wastewater was placed at a height above the level of accumulated soil. This minimized the probability of losing sediments. The effluent water was collected into another container and allowed to settle for 24 h before testing. This ensured that any soil swept into the effluent stream could be returned to the treatment chamber.

After placing the contaminated soil in the treatment chamber, the nanobubble water was filled to half of the height of the chamber. The ultrasound was then applied for the specified time (i.e., 2min, 3min, or 4min, depending on the selected experiment). The probe-typed ultrasound source used in this research had a 1.91 cm tip diameter (Sonic & Materials, Inc., Model Vibracell VC-1500, 240 V, Power 1500 W, and Frequency 20 kHz). Based on the previous experience with optimum power levels, 1200 W was selected for all experiments conducted in this research. At the end of the ultrasound application, the chamber was filled to the full height with nanobubble-saturated water.

Nanobubbles were supplied stepwise because high temperatures caused by the application of ultrasound led to faster ozone depletion, and the higher speed of stirring/movement in the ozone solution resulted in faster decomposition. Thus, both these factors caused a reduction in oxidation efficiency. Therefore, the addition of ozone nanobubbles water to the treatment chamber was carried out in two steps. The first half involved the filling of the chamber and the application of ultrasound to suspend the soil and to desorb contaminants. The second half involved the addition of ozone nanobubbles to facilitate oxidation. Then, the soil was allowed to settle, and the effluent was drained from the treatment chamber. This treatment scheme was repeated until the desired time of ultrasound application, and ozonation was achieved.

At the end of the treatment, sediments were collected into a porcelain container and placed in a temperature-controlled oven at $40\,^{\circ}\text{C}$ until the soil was completely dry. The soil was then allowed to reach room temperature and air-dried for another $24\,\text{h}$ before chemical analysis was performed to determine the removal efficiency.

Chemical analysis. The chemical analysis of soil was performed in two-steps as treated soil contained both organic and inorganic contaminants.

Chemical analysis of p-terphenyl: The USEPA method 3550 B (USEPA, 2007) was used to extract p-terphenyl. Solvent extraction was used to isolate contaminants using enhanced ultrasound in acetone. Accordingly, 20 g of the treated sediment and 100 mL of acetone were mixed in a 250 mL beaker. Sonication was performed in short, 5-s bursts using a 300 W horn-type ultrasound transducer. Short bursts protected the sample from changes in chemical composition and sudden temperature increases. After 10 cycles of sonication, the sample was filtered and collected in a clean 200 mL flask. Then, another cycle of extraction was performed using

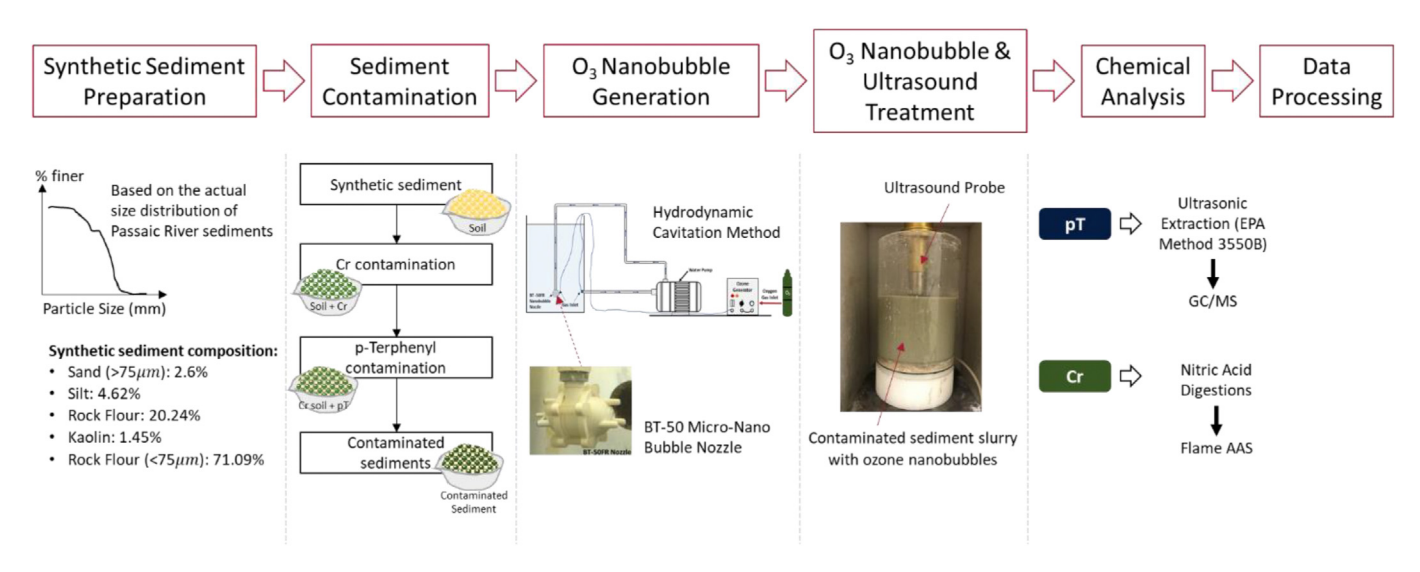


Fig. 2. Schematic flow diagram of the experimental procedure.

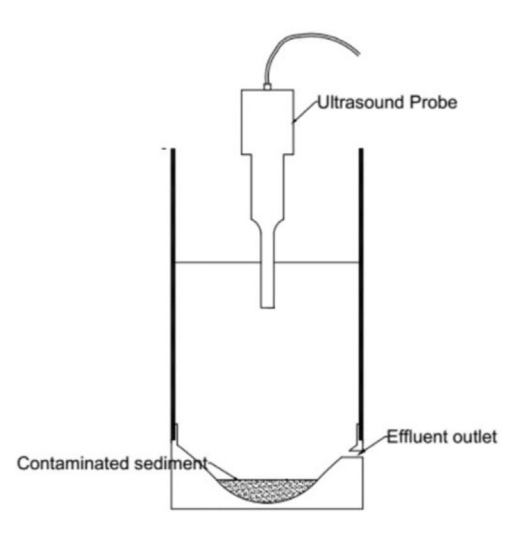




Fig. 3. Contaminated sediment treatment chamber.

another 100 mL of acetone to ensure the complete extraction of contaminants, and the resulting slurry was added to the previously collected sample. The collected 200 mL sample was concentrated using a Kuderna-Danish triple ball concentration column to a volume of 10 mL. The resulting concentrated organic material and acetone were analyzed using gas chromatography with mass spectrometry (GC/MS - Agilent 5973 N) to obtain the contaminant concentration and compute the removal efficiency.

Chemical analysis of chromium: The EPA method number 3050 was used for the sample preparation and Cr analysis. The heavy metal (Cr) was extracted from the 1.0 g of treated dry sediment for the chemical analysis. The 1.0 g sample was digested with 10 mL of trace metal-grade nitric acid (67%—70% w/w). The acid-soil mixture was then heated to 80 °C until the soil sample was completely dissolved in the acid. Then, by adding 990 mL of DI water, this acid-soil solution was diluted. The diluted solutions were tested using flame atomic absorption spectrometry (AAS - PerkinElmer AAnalyst 400) to determine the total element chromium concentration and treatment efficiency. For the analysis, 1 M, 2 M, 3 M, 4 M, and 5 M standard solution was prepared for the calibration.

5. Results and discussion

Size of ozone nanobubbles, zeta potential, and dissolved gas concentration. The determination of chemical and physical characteristics is essential for the successful application of ozone nanobubbles. Consequently, the generated ozone nanobubbles were tested for size distribution and the Zeta Potential values. The Malvern Zetasizer Nano ZS was used to measure the bubble size and Zeta Potential. The Malvern Zetasizer utilizes the Dynamic Light Scattering (DLS) method to measure particle and bubble sizes, and Laser Doppler Micro-electrophoresis is used to measure the Zeta Potential. Fig. 4 shows the (a) size distribution and (b) Zeta Potential values of 48 nanobubble samples obtained over 24 different bubble generations with two duplicates. Those measurements were taken 20 min after nanobubble generation. During the bubble generation, the bubble solution's temperature was increased by an average of 3.06±0.34 $^{\circ}\text{C},$ where the initial was 20 °C.

Fig. 4(a) shows a positively skewed cumulative average size distribution graph, indicating that 75% of the generated bubbles were smaller than 122 nm in diameter. The median of the

distribution was 68.1 nm. In general, the size distribution of the bubbles was recorded between 30 and 300 nm. Treatment efficiency is directly related to the amount of ozone delivered to the system and the half-life of the ozone solution. Based on these factors, the size of the bubble plays a vital role. Smaller bubbles have increased stability due to lower buoyancy force, which prevents faster upward movements. Furthermore, smaller bubbles have a higher specific surface area and hence a larger contact area to react with the pollutants. The nanobubbles have high internal gas pressures, which increases gas diffusion and ozone concentrations at the bubble-liquid interface.

Another critical factor that influences the stability of the nanobubbles is the Zeta Potential. Nanobubbles with high Zeta Potential values prevent the bubbles from merging due to repulsive electrostatic forces. Fig. 4(b) shows the measured Zeta Potential values, and the average Zeta Potential was recorded as -22.77 mV. Higher Zeta Potential would reduce the internal gas pressure to balance the surface tension and increase the life of nanobubbles (Meegoda et al., 2019).

Treatment Efficiencies of Contaminated Sediments: Table 2 shows the experimental parameters and the obtained removal efficiencies. Test IDs O_1 and O_2 show the optimum test results from a previous study where removal efficiencies of 91.5% and 97.5% were obtained for p-terphenyl and chromium, respectively, when there was a single contaminant.

Test IDs from N $_1$ to N $_{13}$ were performed for combined Cr and pterphenyl contaminated soil and tested under different experimental conditions. For each experiment, samples were analyzed 2 times for p-terphenyl using GC/MS and 3 times for chromium using AAS. The relative errors in measurements were minimal, as shown in Table 1, with the standard deviation for Cr was ± 11 mg/kg and for p-terphenyl was ± 4 mg/kg. The recovery of p-terphenyl extracted from sediment was $86 \pm 1\%$, and for chromium, it was $93 \pm 1\%$.

Fig. 5a and b shows Test ID N_1 to N_{13} for test conditions and treatment efficiencies. Fig. 5(a) shows the initial Cr and p-terphenyl concentration and removal efficiencies for each test. Further, it shows the relative contamination levels compared to each test performed in N_1 to N_{13} . Fig. 5(b) shows removal efficiencies for both Cr and p-terphenyl and the average for Test O_1 , O_2 , and N_1 to N_{13} . It also indicates ultrasound energy densities for each test and the number of treatment cycles performed.

Fig. 6 shows selected tests with similar contaminant

Bubble Size (Number Distribution)

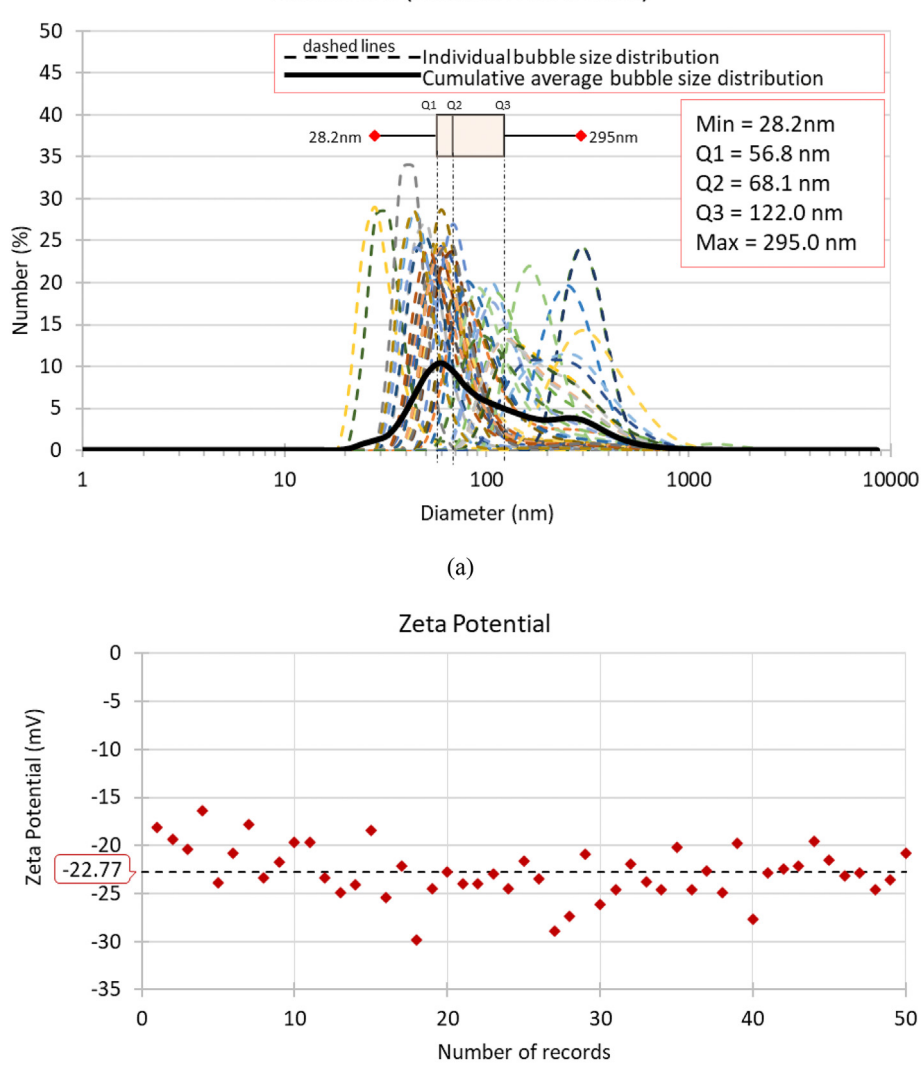


Fig. 4. The characteristics of ozone nanobubbles generated at 20 $^{\circ}$ C and pH \approx 7 (a) size distribution, (b) zeta potential. (48 nanobubble samples obtained over 24 different bubble generations with two duplicates).

(b)

concentrations. It shows that higher ultrasound energy density and the number of treatment cycles improves the overall treatment efficiency. However, it is clear from Fig. 6 that p-terphenyl removal efficiencies are highly dependent on the sonication energy. It shows that the highest removal efficiency for p-terphenyl was 82.7% with 127.2 J/ml energy density. Simultaneously, for Tests N₁, N₂, and N₉, all had similar conditions (Ev: 57.6 J/ml, No. of cycles: 120, and relative ozone usage 100%), yet Test N₉ shows relatively better performance. This improved performance can be attributed to the direct impact of the ultrasound probe with the sediments caused by moving the sediment chamber throughout the sonication cycles. Please note that this condition can be implemented in the chamber shown in Fig. 1 by a higher wastewater extraction rate. For the Cr removal efficiency, the increased energy density had minimal impact, but the increased number of treatment cycles and ozone usage did improve the removal efficeincy of chromium. Fig. 6 shows that the highest removal efficiency for Cr was 87.2% with 78.75/ml energy density.

Fig. 7 shows the comparison between the test results for

different initial contaminant concentrations. Chromium removal efficiencies decreased with increasing concentration of chromium. However, p-terphenyl treatment efficiency shows unexpected results as the decrease in initial p-terphenyl concentration resulted in lower removal efficiencies. It can be related to the pyrolysis of pterphenyl during ultrasound application. When the ultrasound causes the cavitation bubbles to collapse, the chemicals near the collapse site are pyrolyzed. As the p-terphenyl concentration is reduced in the solution, the probability of p-terphenyl contaminated sediment particles reaching the cavitation/reaction zone is reduced, explaining the reduction in the treatment efficiency. Therefore, in the experimental laboratory setup, the p-terphenyl removal efficiencies highly depended on the movement of the sediment chamber during the sonication. Suppose the system is adequately mixed, which allows the sediment particles to reach the reaction zone and get detached or pyrolyze the contaminants. During the sonication, the sediment chamber movement may explain the difference between Test N₁₀ (Chamber moved during the sonication) and N₁₁ (No chamber movement during the

Table 2 Summary of results.

Test	Sonication Parameters (20 kHz, 1200 W)					Amount of Total Ozone water used	Contaminant Type		ntration minant/soi	1)	Removal Efficiency	
		ime duration		Volume/ cycle	Energy Density	uscu	турс					
	Per cycle	No of cycle	Total				_	<u></u>			For Individual Contaminant	Averag
#	(Min)	#	(Min)	(L)	(J/ml)	(L)		(mg/ kg)	(mg/kg)	(mg/kg)	(%)	(%)
O ₁	1 2	_ 120	240	2	72	300	Cr	_	_	_	_	91.5
	3	- -					P-terphenyl	1875	159	1716	91.5	
_	Total	120	2.40	2	70	200	C	2252	01	2172	07.5	07.5
02	1 2	- 120	240	2	72	300	Cr	3253	81	3172	97.5	97.5
	3 4	_					P-terphenyl	_	_	_	_	
N_1	Total 1	120 -	240	2.5	57.6	300	Cr	4211	1242±20	2969	70.5	61.7
	2	120 -					P-terphenyl	1875	885	990	52.8	
	4	_					r-terphenyi	1075	003	330	32.8	
N_2	Total 1	120 -	240	2.5	57.6	300	Cr	4211	1209±30	3002	71.3	61.8
2	2	120	2.10	2.0	57,10	300						01.0
	3 4	_					P-terphenyl	1875	896±8	979	52.2	
N I	Total	120 -	240	2	72	300	Cr	4211	1204 . 12	2027	69.5	70.9
N ₃	1 2	120	240	2	12	300	Ci	4211	1284±12	2927	09.5	70.9
	3 4	_					P-terphenyl	1875	519	1356	72.3	
	Total	120										
N ₄	1 2	_	424	2	127.2	300	Cr	4211	1108±22	3103	73.7	78.2
	3 4	56					P-terphenyl	1875	324	1551	82.7	
	4 Total	64 120										
N ₅	1 2	20 _	320	2	96	300	Cr	2106	495±11	1610	76.5	75.1
	3	100 —					P-terphenyl	937.5	238±10	699.5	74.7	
N ₆	Total	120 53	262	2	78.75	320	Cr	1840	354±9	1486	80.8	73
146	2	25	202	2	76.75	520	Ci	1040	334 <u>±</u> 3	1400	80.8	/5
	3 4	23 27					P-terphenyl	937.5	326	611.5	65.2	
	Total	128										
N ₇	1 2	53 25	262	2	78.75	320	Cr	1227	157±14	1070	87.2	69.3
	3 4	23 27					P-terphenyl	625	304	321	51.3	
	Total	128										
N ₈	1 2	0 150	300	2.5	57.6	375	Cr	4211	965±34	3246	77.1	75.2
	3	0					P-terphenyl	1875	492 ± 4	1383	73.8	
	4 Total	0 150										
N ₉	1 2	0 120	240	2.5	57.6	300	Cr	4211	1168±33	3032	72.0	66.4
	3	0					P-terphenyl	1875	737±9	1138	60.7	
	4 Total	0 120										
N ₁₀		0	240	2.5	57.6	300	Cr	2770	1040±19	1730	62.5	67.9
	2	120 0					P-terphenyl	937.5	251±14	686.5	73.2	
	4 Total	0 120										
N ₁₁	1	0	240	2.5	57.6	300	Cr	2770	1320±34	1450	52.3	53.9
	2	120 0					P-terphenyl	937.5	418.5	519	55.4	
	4	0										
N ₁₂	Total 1	120 0	240	2.5	76.8	405	Cr	3323	991±38	2332	70.2	63.0
	2 3	60										
	3	0					P-terphenyl	1875	830	1045	55.7	

Table 2 (continued)

Test Sonication Parameters (20 kHz, 1200 W)) W)	Amount of Total Ozone water					Removal Efficiency	
			Volume/	Energy	used	Type	(contaminant/soil)					
	Per cycle	No of cycle	Total	cycle Density			Initial	Residual	Removal	For Individual Contaminant	Average	
#	(Min)	#	(Min)	(L)	(J/ml)	(L)		(mg/ kg)	(mg/kg)	(mg/kg)	(%)	(%)
	4 Total	30 90		_					_			
N ₁₃	1 2	0 60	240	2.5	76.8	405	Cr	3323	980±10	2343	70.5	63.0
	3	0 30					P-terphenyl	1875	761	1114	59.4	
	Total	90										

sonication) results, while all the other parameters were identical. In practical applications, this factor should be carefully addressed by appropriately adjusting the wastewater extraction rate from the treatment chamber shown in Fig. 1 so that ultrasound energy is uniformly and effectively distributed in the chamber.

In Tests N₁₂ and N₁₃, additional amounts of ozone saturated water volume were added compared to other experiments. These tests also had a relatively high energy density of 76.8 J/ml, and sonication was performed for 240 min in only 90 cycles (2min pulse for 60 cycles and 4 min pulse of 30 cycles). Although the additional amount of ozone was added to the system, the reduction in treatment cycles profoundly impacted the removal efficiency of p-terphenyl. Tests N₁₂ and N₁₃ indicate that the importance of washing cycles on treatment efficiency. To summarize, the p-terphenyl removal efficiency increased with an increased ozone availability but was mainly impacted by the ultrasound energy and the number of treatment cycles. By selecting higher energy densities and increasing the number of treatment cycles, p-terphenyl degradation can be optimized. According to the GC-MS data, the tested wastewater showed minimal to no daughter byproducts; hence, complete mineralization of p-terphenyl was expected.

When the overall experimental results were compared from all tests, chromium removal efficiencies were held nearly constant, around 71%, showing no impact on the increase in ultrasound energy. Because the currently applied ultrasound energies contribute to the best possible chromium removal, an additional increase does not contribute to further improvements but can reduce removal efficiency as higher ultrasound power can reduce the ozone concentration in the solution. Results indicate that the available ozone directly impacted the chromium removal efficiency. Therefore, to improve the chromium removal efficiency, the number of treatment cycles, and the ozone concentration in the solution should be increased while desired ultrasound power levels are maintained at similar levels.

Based on the above observations, Cr removal is directly influenced by the chemical oxidation and sonication for Cr detachments. P-terphenyl degradation is more likely influenced by the combined effects of oxidation and ultrasound-assisted pyrolysis.

Heavy metals are not degradable pollutants. Therefore, to completely remove Cr from the system, wastewater containing Cr needs to be extracted from the sediment-water mixture. Hence in this process, as the Cr(III) is firmly bonded onto sediment particles, it needs complete oxidation into Cr(VI), the water-soluble phase, where it is then extracted out by several cycles of washing out with ozonated water.

Other researchers have reported that the degradability of organic contaminants decreased with heavy metals in the

sediments. The organic pollutant biodegradability and their biodegradation rate decreased with heavy metals in the environment and, therefore, doubled the environmental pollution (Masindi and Muedi, 2018).

The sorption process influences the interaction of organic contaminants with sediments (Karickhoff et al., 1979). The sorption to soil and sediments act as the most influential factor in the transportation and fate of organic contaminants in the environment (Chiou and Kile, 2000). The sediment and organic pollutant sorption process are driven by van der Waals interactions, electrostatic interactions, π -bonding, hydrogen bonding, ligand exchange reactions, dipole-dipole interaction, and chemisorption (Wuana et al., 2014). The hydrophobic effect of pollutants mainly drives the sorption of organic contaminants into sediments. Under natural conditions, soil or sediments have minerals and organic matter attached to them, which significantly influences the sorption process. The soil or sediment with organic matter (SOM) works as a dual-function sorbent, where the mineral matter sorbs the contaminant by adsorption, while the SOM sorbs the contaminant by a partition (Chiou and Kile, 2000).

Heavy metals in the soil/sediments in nature mainly occur in immobile forms and are primarily bound with silicate minerals and secondarily to clay minerals (Wuana et al., 2014). When the heavy metal contaminates the soil due to external sources, the contaminants are not always attached to silica bounds or clay minerals in sediments. Therefore, they are weekly bonded to sediments and are environmentally available and toxic, impacting humans, and natural habitats. There are five types of heavy metal binding to accumulate metals in sediments: 1) adsorptive and exchangeable, 2) bound to carbonates, 3) bound to organic matter and sulfides, 4) bound to Fe and Mn oxides, and 5) residual metals (Lin and Chen, 1998).

With combined contamination of organic and inorganic contaminants, the overall response may differ from that for each contaminant acting independently. Results showed that sediments mixed with p-terphenyl and Cr had increased the overall bonds with sediments and decreased the removal efficiency. This proposed treatment method shows sufficient remediation success with removing these combined contaminants, on average, 60% and 71% for p-terphenyl and chromium, respectively based on the average of N1, N2, N3, and N9, which used 240min ultrasound, and initial Cr concentration of 4211 mg/kg and initial p-terphenyl concentration of 1875 mg/kg. The test results show highest removal efficiency for p-terphenyl was 82.7% and that for Cr was 87.2% with 127.2 J/ml and 78.75/ml energy densities repactively, whereas 91.5% and 97.5% removal efficiencies were obtained for the same, respectively, as a single contaminant in the sediment. Therefore, p-

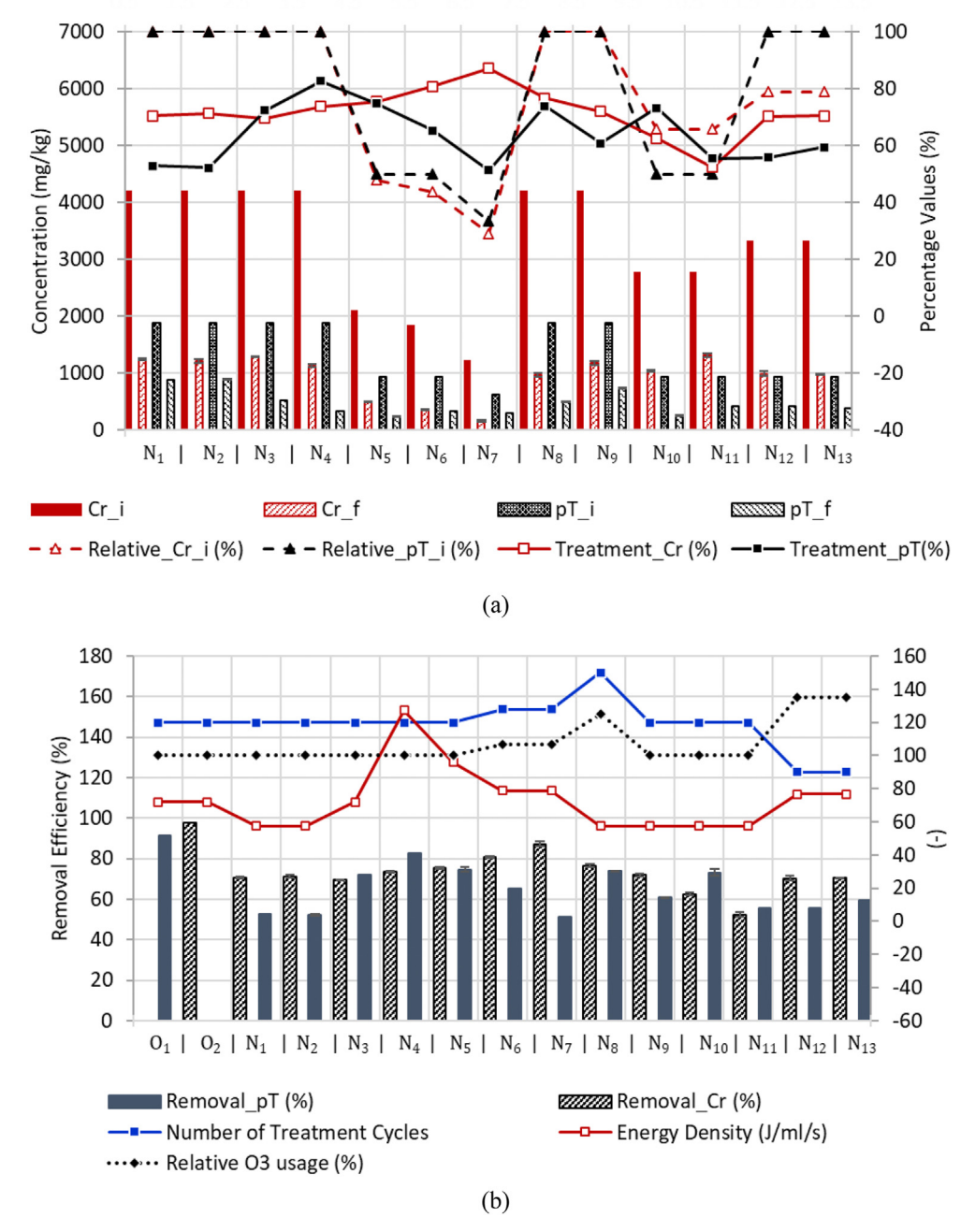


Fig. 5. Summary of the calculated values for each test performed (a) Part A and b (Part B).

terphenyl degradability and chromium extractability has been reduced with combined contamination causing lower removal efficiencies when compared to the treatment of soil/sediment contaminated with an individual contaminant.

The next step of this research would be to evaluate this treatment technology using actual contaminated sediments obtained from the lower Passaic River and develop an in situ treatment device (Aluthgun Hewage et al., 2020; Batagoda et al., 2018; Meegoda et al., 2017a) for possible field implementation. Concurrently, the authors are also exploring the feasibility of high and low-frequency ultrasound to remediate lower Passaic River sediments without using ozone nanobubbles (Meegoda and Kewalramani, 2020).

6. Summary and conclusions

This research evaluated an in-situ sediment remediation method using ultrasound and ozone nanobubbles to remediate both organic and inorganic chemicals in contaminated sediments to be applied to remediate contaminated sediments from the lower Passaic River. Sediment contaminated with both Cr and p-terphenyl were subjected to different experimental conditions. This proposed treatment method shows sufficient remediation success with removing these combined contaminants, on average, 60% and 71% for p-terphenyl and chromium, respectively. According to the obtained results, the Cr removal is directly influenced by the chemical oxidation and sonication for Cr desorption from sediments. While p-terphenyl degradation was more likely influenced by the

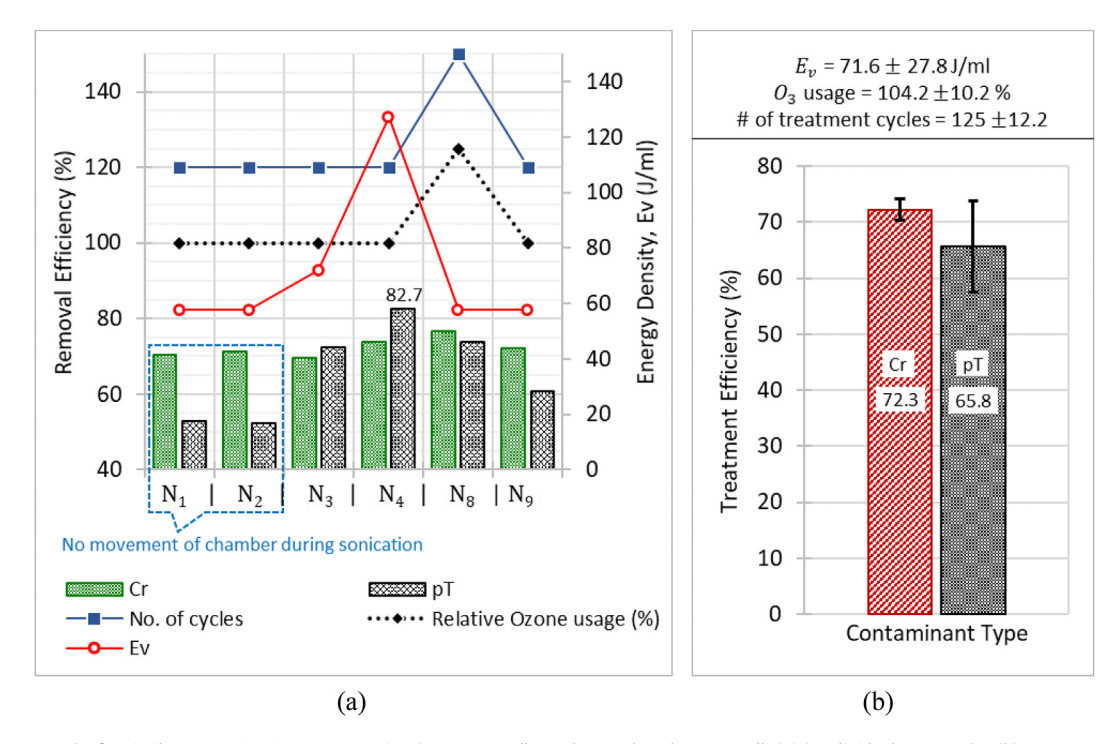


Fig. 6. Test results for similar contamination concentration (Cr: 4211 mg/kg and p-terphenyl: 1875 mg/kg) (a) Individual test results, (b) Average test results.

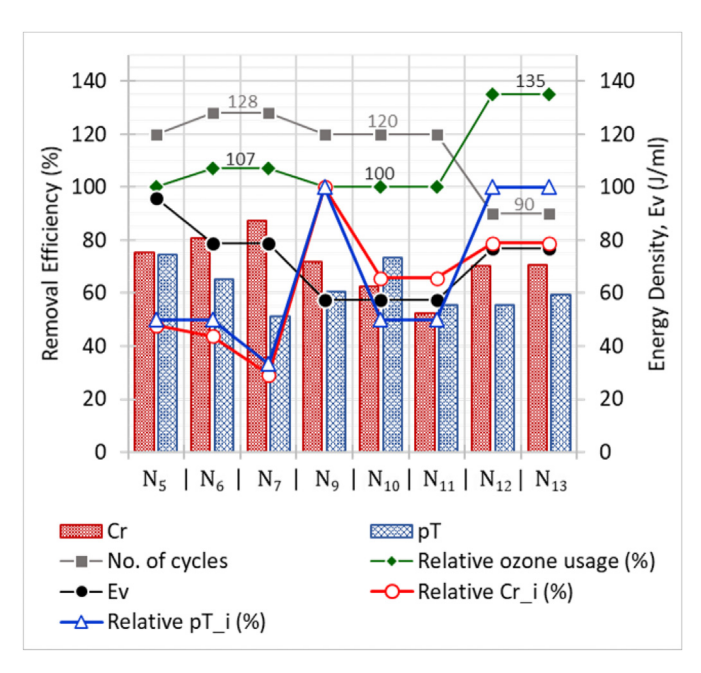


Fig. 7. Effect of the initial concentration of contaminants.

combined effects of chemical oxidation and ultrasound-assisted pyrolysis. These contaminant removal rates can be improved by increasing the amount of ozone added to the system and increasing the washout cycles. The increase in sonication time can also improve treatment efficiency but would increase energy costs. Further, this method may be evaluated by combining with proper catalysis and using different ultrasound frequencies or multiple ultrasound sources. The chemical oxidation improvement through increasing the hydroxyl radical in the system would benefit the proposed method. Hence, research will continue to evaluate ways

to improve removal efficiency by changing the oxidation agents. This treatment method seems promising but requires additional investigation to improve and optimize the treatment to lower energy cost and time.

Credit author statement

Shaini Aluthgun Hewage, Conceptualization, Formal analysis, Investigation, Writing — original draft, Writing — review & editing, Visualization. Janitha Hewa Batagoda, Conceptualization, Methodology. Jay Meegoda, Conceptualization, Methodology, Resources, Writing — original draft, Writing — review & editing, Supervision, Project administration, Funding acquisition.

Declaration of competing interest

The authors declare that they have no known competing financial interests or personal relationships that could have appeared to influence the work reported in this paper.

Acknowledgments

This research was sponsored by the US National Science Foundation Award #1634857 entitled "Remediation of Contaminated Sediments with Ultrasound and Ozone Nanobubbles." The program manager at NSF was Dr. Richard Fragaszy and now Dr. Joy Pauschke. The authors would like to acknowledge the contributions of Mr. Brian McGlew, an undergraduate student of NJIT, and Mr. Natan Herzog, a high school student from Bergen County Technical High School – Teterboro. The authors would also like to acknowledge the efforts of four anonymous reviewers whose efforts substantially improved the presentation.

References

Agarwal, A., Ng, W.J., Liu, Y., 2011. Principle and applications of microbubble and nanobubble technology for water treatment. Chemosphere. https://doi.org/

- 10.1016/j.chemosphere.2011.05.054.
- Aluthgun Hewage, S., Batagoda, J.H., Meegoda, J.N., 2020. In situ remediation of sediments contaminated with organic pollutants using ultrasound and ozone nanobubbles. Environ. Eng. Sci. 37, 521–534. https://doi.org/10.1089/ees.2019.0497.
- Batagoda, J.H., Hewage, S.D.A., Meegoda, J.N., 2019. Remediation of heavy-metal-contaminated sediments in USA using ultrasound and ozone nanobubbles. J. Environ. Eng. Sci. 14, 130–138. https://doi.org/10.1680/jenes.18.00012.
- Batagoda, J.H., Hewage, S.D.A., Meegoda, J.N., 2018. Nano-ozone bubbles for drinking water treatment. J. Environ. Eng. Sci. 14, 57–66. https://doi.org/10.1680/jenes.18.00015.
- Chaplin, M., 2019. Water structure and science: nanobubbles (ultrafine bubbles) [WWW Document]. URL. http://www1.lsbu.ac.uk/water/nanobubble.html.
- Chen, D., Sharma, S.K., Mudhoo, A. (Eds.), 2011. Handbook on Applications of Ultrasound, Handbook on Applications of Ultrasound. CRC Press. https://doi.org/10.1201/b11012.
- Chiou, C.T., Kile, D.E., 2000. Contaminant sorption by soil and bed sediment—is there a difference? U.S. Geol. Surv. Fact Sheet 087-00 4.
- Ebina, K., Shi, K., Hirao, M., Hashimoto, J., Kawato, Y., Kaneshiro, S., Morimoto, T., Koizumi, K., Yoshikawa, H., 2013. Oxygen and air nanobubble water solution promote the growth of plants, fishes, and mice. PloS One 8. https://doi.org/ 10.1371/journal.pone.0065339.
- Eriksson, M., 2005. Ozone Chemistry in Aqueous Solution Ozone Decomposition and Stabilisation. Technology.
- Flint, E.B., Suslick, K.S., 1991. The temperature of cavitation. Science 84 253, 1397–1399. https://doi.org/10.1126/science.253.5026.1397.
- Hewa Batagoda, J., 2018. Decontamnination of the Passaic River Sediments Using Ultrasound with Ozone Nano-Bubble. New Jersey Institute of Technology.
- Hewage, S.A., Kewalramani, J., Meegoda, J.N., 2021. Stability of nanobubbles in different salts solutions. Colloids Surfaces A Physicochem. Eng. Asp. 609, 125669. https://doi.org/10.1016/j.colsurfa.2020.125669.
- Hu, L., Xia, Z., 2018. Application of ozone micro-nano-bubbles to groundwater remediation. J. Hazard Mater. 342, 446–453. https://doi.org/10.1016/ j.jhazmat.2017.08.030.
- Kamolpornwijit, W., Batagoda, J.H., Meegoda, J.N., 2018. Optimisation of metal extraction from chromium ore processing residue in New Jersey, USA. J. Environ. Eng. Sci. 13, 98–107. https://doi.org/10.1680/jenes.18.00009.
- Kamolpornwijit, W., Meegoda, J.N., Batagoda, J.H., 2015. Engineering properties of chromium contaminated soils. Geotech. Eng. 46, 8–15.
- Karickhoff, S.W., Brown, D.S., Scott, T.A., 1979. Sorption of hydrophobic pollutants on natural sediments. Water Res. 13, 241–248. https://doi.org/10.1016/0043-1354(79)90201-X.
- Krishnan, S., Rawindran, H., Sinnathambi, C.M., Lim, J.W., 2017. Comparison of various advanced oxidation processes used in remediation of industrial wastewater laden with recalcitrant pollutants. In: IOP Conference Series: Materials Science and Engineering. https://doi.org/10.1088/1757-899X/206/1/ 012089
- Kewalramani, J.A., Zou, Z., Marsh, R.W., Bukiet, B.G., Meegoda, J.N., 2020. Nonlinear behavior of high-intensity ultrasound propagation in an ideal fluid. Acoustics. https://doi:10.3390/acoustics2010011.
- Kuppusamy, S., Palanisami, T., Megharaj, M., Venkateswarlu, K., Naidu, R., 2016. Exsitu remediation technologies for environmental pollutants: a critical perspective. In: Reviews of Environmental Contamination and Toxicology, pp. 117–192. https://doi.org/10.1007/978-3-319-20013-2_2.
- Lin, J.G., Chen, S.Y., 1998. The relationship between adsorption of heavy metal and organic matter in river sediments. Environ. Int. 24, 345–352. https://doi.org/ 10.1016/S0160-4120(98)00012-9.
- Liu, S., Kawagoe, Y., Makino, Y., Oshita, S., 2013. Effects of nanobubbles on the physicochemical properties of water: the basis for peculiar properties of water containing nanobubbles. Chem. Eng. Sci. 93, 250–256. https://doi.org/10.1016/ ices.2013.02.004
- Loeb, B.L., Thompson, C.M., Drago, J., Takahara, H., Baig, S., 2012. Worldwide ozone capacity for treatment of drinking water and wastewater: a review. Ozone Sci. Eng. 34, 64–77. https://doi.org/10.1080/01919512.2012.640251.
- Louis Berger Group, I., 2014. Remedial Investigation Report for the Focused

- Feasibility Study of the Lower Eight Miles of the Lower Passaic River.
- Masindi, V., Muedi, K.L., 2018. Environmental contamination by heavy metals. In: Heavy Metals. InTech. https://doi.org/10.5772/intechopen.76082.
- Meegoda, J.N., Perera, R., 2001. Ultrasound to decontaminate heavy metals in dredged sediments. J. Hazard Mater. 85, 73–89. https://doi.org/10.1016/S0304-3894(01)00222-9.
- Meegoda, J.N., Veerawat, K., 2002. Ultrasound to decontaminate organic compounds in dredged sediments" soil & sediment contamination. Int. J. 11, 91–116.
- Meegoda, J.N., Aluthgun Hewage, S., Batagoda, J.H., 2018. Stability of nanobubbles. Environ. Eng. Sci. 35, 1216–1227. https://doi.org/10.1089/ees.2018.0203.
- Meegoda, J.N., Aluthgun Hewage, S., Batagoda, H.J., 2019. Application of the diffused double layer theory to nanobubbles. Langmuir 35 (37), 12100—12112. https://doi.org/10.1021/acs.langmuir.9b01443.
- Meegoda, J.N., Batagoda, J.H., Aluthgun-Hewage, S., 2017a. Briefing: in situ decontamination of sediments using ozone nanobubbles and ultrasound. J. Environ. Eng. Sci. 12, 1–3. https://doi.org/10.1680/jenes.17.00006.
- Meegoda, J.N., Kamolpornwijit, W., Batagoda, J.H., 2017b. A detailed laboratory scale feasibility study of recovering metallic iron and chromium from chromium contaminated soils. Indian Geotech. J. 47, 437–444. https://doi.org/10.1007/ s40.098-016-0208-4.
- Meegoda, J.N., Kewalramani, J., 2020. Coupled High and Low Frequency Ultrasonic for Destruction of Organics. US Provisional Patent Application. # 62/965,346.
- Onwueme, V., Feng, H., 2006. Risk characterization of conatmainats in Passaic River sediments, New Jersey. Middle States Geographer 39, 13–25.
- Rasalingam, S., Peng, R., Koodali, R.T., 2014. Removal of hazardous pollutants from wastewaters: applications of TiO 2-SiO2 mixed oxide materials. J. Nanomater. 1–42. https://doi.org/10.1155/2014/617405.
- Richard, F.C., Bourg, A.C.M., 1991. Aqueous geochemistry of chromium: a review. Water Res. 25, 807–816. https://doi.org/10.1016/0043-1354(91)90160-R. Sharma, A., Ahmad, J., Flora, S.J.S., 2018. Application of advanced oxidation pro-
- Sharma, A., Ahmad, J., Flora, S.J.S., 2018. Application of advanced oxidation processes and toxicity assessment of transformation products. Environ. Res. 167, 223–233. https://doi.org/10.1016/j.envres.2018.07.010.
- Teefy, D.A., 1997. Remediation Technologies Screening Matrix and Reference Guide: Version III, Remediation. https://doi.org/10.1002/rem.3440080111.
- Thomé, A., Reginatto, C., Vanzetto, G., Braun, A.B., 2019. Remediation technologies applied in polluted soils: new perspectives in this field. In: Environmental Science and Engineering., pp. 186–203. https://doi.org/10.1007/978-981-13-2221-1 11.
- USEPA, 1991. Handbook Remediation of Contaminated Sediments. EPA, Cincinnati, OH
- USEPA, 2006. Situ Treatment Technologies for Contaminated Soil. Situ.
- USEPA, 2007. Ultrasonic extraction. EPA method 3550C 1-17.
- USEPA, 2014a. Fact Sheets: the Passaic River's Polluted Past. United States Environ. Prot. Agency.
- USEPA, 2014b. Memorandum to Diane Salkie, Remedial Project Manager, Region 2. CSTAG Recommendations on the Lower Passaic River Study Area, 17 Mile Remedial Investigation/Feasibility Study and Proposed Interim Remedial Action. United States Environ. Prot. Agency.
- USEPA, 2019. What is sediment pollution? Mid-America reg. Councilor 1–2.
- Ushikubo, F.Y., Furukawa, T., Nakagawa, R., Enari, M., Makino, Y., Kawagoe, Y., Shiina, T., Oshita, S., 2010. Evidence of the existence and the stability of nanobubbles in water. Colloids Surfaces A Physicochem. Eng. Asp. 361, 31–37. https://doi.org/10.1016/j.colsurfa.2010.03.005.
- Wuana, R. a, Okieimen, F.E., Vesuwe, R.N., 2014. Mixed contaminant interactions in soil: implications for bioavailability, risk assessment and remediation. Afr. J. Environ. Sci. Technol. 8, 691–706.
- Yang, G., Zhu, J.J., 2016. Sonoelectrochemical synthesis and characterization of nanomaterials #10. In: Handbook of Ultrasonics and Sonochemistry. Springer Singapore, Singapore, pp. 295–324. https://doi.org/10.1007/978-981-287-278-4_11.
- Yong, R.N., 1995. Fate of toxic pollutants in contaminated sediments. In: ASTM Special Technical Publication. ASTM International, 100 Barr Harbor Drive, West Conshohocken, pp. 13–27. https://doi.org/10.1520/STP15989S. PO Box C700.
- Young, F.R., 1999. Cavitation. Imperial College Press. https://doi.org/10.1142/p172.